




Ecosystem productivity has a stronger influence than soil age on surface soil carbon storage across global biomes

César Plaza ^{1✉}, Pablo García-Palacios¹, Asmeret Asefaw Berhe ², Jesús Barquero³, Felipe Bastida⁴, G. Kenny Png^{5,6}, Ana Rey⁷, Richard D. Bardgett⁵ & Manuel Delgado-Baquerizo ^{8,9✉}

Interactions between soil organic matter and minerals largely govern the carbon sequestration capacity of soils. Yet, variations in the proportions of free light (unprotected) and mineral-associated (protected) carbon as soil develops in contrasting ecosystems are poorly constrained. Here, we studied 16 long-term chronosequences from six continents and found that the ecosystem type is more important than soil age (centuries to millennia) in explaining the proportion of unprotected and mineral-associated carbon fractions in surface soils across global biomes. Soil carbon pools in highly productive tropical and temperate forests were dominated by the unprotected carbon fraction and were highly vulnerable to reductions in ecosystem productivity and warming. Conversely, soil carbon in low productivity, drier and colder ecosystems was dominated by mineral-protected carbon, and was less responsive to warming. Our findings emphasize the importance of conserving ecosystem productivity to protect carbon stored in surface soils.

¹Instituto de Ciencias Agrarias (ICA), CSIC, Serrano 115 bis, 28006 Madrid, Spain. ²Department of Life and Environmental Sciences and Sierra Nevada Research Institute, University of California Merced, Merced, CA 95343, USA. ³Departamento de Sistemas Físicos, Químicos y Naturales, Universidad Pablo de Olavide, 41013 Sevilla, Spain. ⁴CEBAS-CSIC, Department of Soil and Water Conservation, Campus Universitario de Espinardo, 30100 Murcia, Spain. ⁵Department of Earth and Environmental Sciences, Michael Smith Building, The University of Manchester, Oxford Road, Manchester M13 9PT, UK. ⁶Asian School of the Environment, Nanyang Technological University, 50 Nanyang Avenue, Singapore 639798, Singapore. ⁷Departamento de Biogeografía y Cambio Global, Museo Nacional de Ciencias Naturales (MNCN), CSIC, Serrano 115 bis, 28006 Madrid, Spain. ⁸Laboratorio de Biodiversidad y Funcionamiento Ecosistémico, Instituto de Recursos Naturales y Agrobiología de Sevilla (IRNAS), CSIC, Av. Reina Mercedes 10, E-41012 Sevilla, Spain. ⁹Unidad Asociada CSIC-UPO (BioFun), Universidad Pablo de Olavide, 41013 Sevilla, Spain. ✉email: cesar.plaza@csic.es; M.DelgadoBaquerizo@gmail.com

Surface soil carbon (C) in the form of organic matter supports essential ecosystem services such as climate regulation, plant production, nutrient cycling and water storage and purification^{1–5}. Global data show that soil C content is larger in cold and mesic than in warm and xeric ecosystems⁶. Moreover, we know that soil C often accumulates during the first thousands of years of ecosystem development⁷, and declines during ecosystem retrogression over millennia⁸. Soil C gains and losses are driven by intertwined changes in primary productivity and stabilization and destabilization processes, which in turn are in part governed by the interaction of soil organic matter with minerals^{1,9}. Specifically, the long-term preservation of soil C is mediated by occlusion within aggregates and by the formation of organo-mineral associations^{10,11}, which limit the accessibility of microorganisms and their extracellular enzymes to the organic substrates and increasing energy requirements for respiration^{9,12–14}. Thus, the mineral-associated C fraction of soil organic matter may be less vulnerable to microbial decomposition, and consequently to warming-induced-increases of microbial respiration, than the particulate and free light C fractions, which are largely unprotected by minerals^{15–17}.

The mineral control of soil C accumulation and loss has been highlighted in recent studies across large temporal^{11,18,19} and spatial gradients^{20,21}. For example, studies conducted on single chronosequences in Hawaii and California have found positive relationships between soil C and mineral reactivity, and suggested that weathering first increases and subsequently reduces the potential of soil to stabilize C^{9,19}. This pattern is particularly evident in soils where short-range order and non-crystalline minerals form in relatively large amounts^{22–24}. Despite these important advances, we still lack a comprehensive understanding of how, why and to what extent the mineral protection of C (assessed by the proportion of soil C in mineral-associated vs. free fractions) changes as soil develops over centuries to millennia across different ecosystems. Such fundamental knowledge is crucial to improve our understanding of soil C storage and turnover over large spatiotemporal scales, reduce uncertainties in the representation of soil processes in land C models, and ultimately shape land management strategies to foster the multiple ecosystem services of soil organic matter, including climate regulation. Most studies to date on this topic have been based on single chronosequences^{9,19,25,26}. Here, we advance on this by exploring the major drivers of soil organic C fractionation as soil develops across 16 globally distributed soil chronosequences from contrasting ecosystems. The objective of this work was to determine how and why the amount and the proportion of surface (0–10 cm) soil C stored in different organic matter fractions changes during soil development across biomes.

These chronosequences cover a range of parent material (volcanic material, sedimentary rocks, and sand dunes) and ecosystems (from deserts to tropical forests and croplands; Supplementary Fig. 1 and Supplementary Data 1)²⁷. Within each soil chronosequence, we selected four to six stages ranging from hundreds to millions of years sharing similar parent material and climate. We applied a density-based, soil organic matter fractionation to separate and quantify soil organic C content in three distinct fractions based on their association with minerals: free light fraction (not protected by minerals); occluded light fraction (protected by occlusion within aggregates); and mineral-associated fraction (protected by sorption to minerals)²⁸. Using this information, we calculated the proportion of organic C stored in each fraction in relation to the total organic C content (proportion of organic C fraction i = organic C fraction i content \times 100/sum of all organic C fraction contents). We focused on the surface soil (top 10 cm, after removing any litter/plant debris on the soil surface) because it is the most biologically active layer and

the most exposed to environmental factors, as well as because the surface soil C is especially relevant to support soil functioning and multiple environmental services^{1,29}. This sampling depth is also consistent with previous studies on soil C storage across spatio-temporal scales^{19,21,30}. Additional details on methods are in Appendix S1: Section S1.

Results and discussion

Changes in C fractions during soil development. Total C stocks in the surface soil were generally largest in grasslands and forests, specifically in temperate and tropical regions (Supplementary Fig. 2). Moreover, soil C stocks in these ecosystems generally tracked a hump-shaped relationship with soil age, with the largest stocks occurring at intermediate stages of soil development (Supplementary Fig. 2). This relationship agrees with results from single-chronosequence studies on soils relatively dominated by short-range order and non-crystalline minerals^{9,18,19,22,23}. We further show that the free light and mineral-associated fractions consistently dominated the soil C stocks across chronosequences (Fig. 1 and Supplementary Fig. 3), while the occluded light fraction only represented a minor part (less than 10% on average across chronosequence sites). Because of this, we focused on the free light and mineral-associated C fractions for downstream analyses. We also focused our discussion mainly on the proportion of soil C stored in each fraction rather than changes in stocks, because the quantification of the latter would require no changes in soil bulk density through time³¹, and this condition was not met in our chronosequences.

Our data revealed that while the mineral protection of soil C differed vastly across ecosystems, it changed to a much lesser extent during soil development within each chronosequence (Fig. 1). In fact, these results were confirmed by linear mixed-effects modeling (see Methods for details), which revealed that ecosystem productivity significantly alters the proportion of organic C in the free light ($p = 0.002$) and mineral-associated ($p = 0.005$) fractions across chronosequences but soil age class (i.e., thousands of years, hundreds of thousand years and millions of years) does not ($p > 0.05$; Supplementary Fig. 4). In particular, warm and wet tropical and temperate (e.g., subtropical and Mediterranean) ecosystems (often forests) had a consistently larger proportion of free light relative to mineral-associated C fraction irrespective of soil age (7/8 chronosequences, 35/45 plots; Fig. 1 and Supplementary Fig. 3). These tropical and temperate ecosystems also had relatively larger contents of soil organic C (Supplementary Figs. 2, 3 and 5). In contrast, in arid and cold ecosystems with less primary production (e.g., desert shrublands), most organic C was stored in the mineral-associated fraction (7/8 chronosequences and 29/42 plots; Fig. 1 and Supplementary Figs. 2, 3 and 5). The chronosequences from Arizona (AZ) and Hawaii (HA) illustrate the point that mineral protection of surface soil organic C varies more between than within ecosystems as soil develops from centuries to millennia. Both forest ecosystems are on volcanic substrates and developed over the same period (3–4 million years), yet the semiarid ecosystem from AZ is, on average, dominated by the mineral-associated C fraction (56%), while the tropical ecosystem from HA is permanently dominated by the free light fraction (average proportion of mineral-associated C <2%; Fig. 1 and Supplementary Data 1). Similarly, cold grasslands from Colorado (CO), which developed over millennia on sedimentary substrates, were dominated by the mineral-associated C fraction (61%), while comparable, but warmer, ecosystems from California (CAL) were dominated by the free light fraction (35% of mineral-associated C on average; Fig. 1 and Supplementary Data 1).

The C distribution found in two soil chronosequences contrasted with the cold and arid vs. warm and wet ecosystem

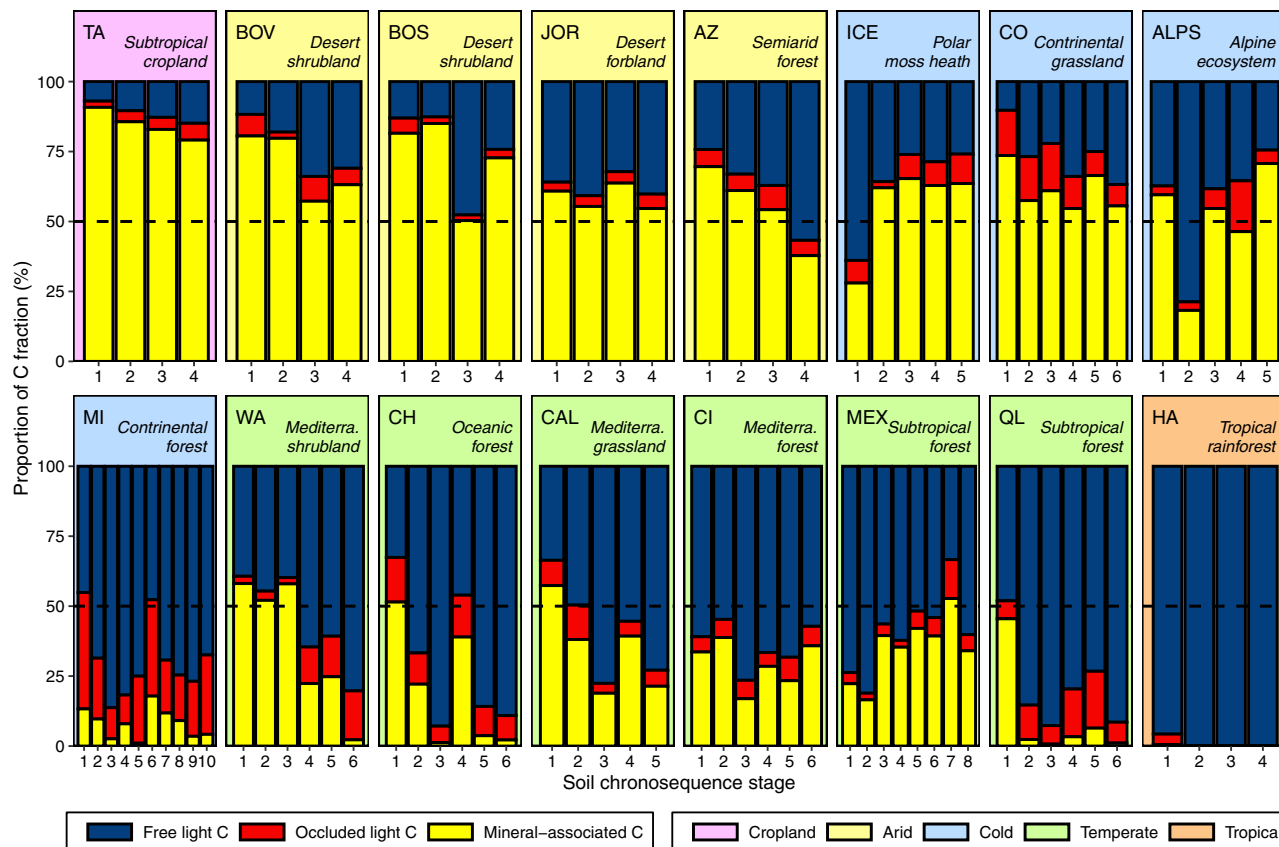


Fig. 1 Proportion of carbon fractions in surface soil organic matter during ecosystem development. Changes in the relative abundance of free light, occluded light and mineral-associated carbon (C) fractions in surface soil organic matter during ecosystem development across 87 sites from 16 globally distributed soil chronosequences. Dashed line indicates 50%. Proportion of C fraction i (%) was calculated as $C \text{ fraction } i \text{ content} \times 100 / \text{sum of all C fraction contents}$. The soil chronosequences are ordered by major biomes: croplands, arid, continental (cold), temperate and tropical ecosystems according to the Koppen classification³⁸. Additional statistical analyses and alternative representation of these data can be found in Supplementary Figs. 3 and 4. See text and Supplementary Data 1 for more information on the chronosequences.

pattern regarding the dominance of C stored in the mineral-associated vs. free light organic matter fractions. In particular, soil C in the chronosequence located in a highly productive continental forest in North America (MI, 10 plots) was predominantly stored in free light organic matter, rather than in the mineral-associated organic matter fraction as was found in the other cold ecosystems (Fig. 1 and Supplementary Fig. 3). Conversely, soil C contents of a subtropical soil chronosequence cropped with tea for the last 100 years in an area naturally dominated by broad-leaved evergreen forests in Taiwan (TA, 4 plots)³² were much smaller (Supplementary Fig. 2) than those found in other productive and warm ecosystems (e.g., Queensland, QL, Mexico, MEX, and Hawaii, HA; Supplementary Fig. 2), and were also dominated by mineral-associated rather than free light organic matter fractions (Fig. 1 and Supplementary Fig. 3). Overall, these local contingencies lend support to the global pattern reported here, supporting the importance of free light organic matter as a dominant C pool in the soil of undisturbed forest ecosystems. In addition, these results suggest that land use conversion of broad-leaved evergreen forest to agriculture in the TA chronosequence altered the millennial balance of C contents, resulting in relevant losses of unprotected C fractions from the soil.

The proportion of surface soil C stored in free light organic matter was positively correlated with microbial respiration rates, whereas the opposite was found for the proportion of mineral-associated C (Fig. 2). An additional experiment across a subset of eight chronosequences that represented all the major biomes

examined here revealed a positive relationship between the proportion of C stored in the free organic matter fraction and the temperature sensitivity of soil respiration (i.e., evaluated with the Q_{10} coefficient as the increase in soil respiration with a temperature increase of 10 °C; Fig. 2).

Together, these findings suggest that surface soil C dominated by the free C fraction, mainly associated with temperate and tropical ecosystems in our chronosequence network, is relatively more vulnerable to microbial decomposition and dependent on temperature increases. This is consistent with recent observations demonstrating a surprisingly high temperature sensitivity of soil C in tropical forests that may result in substantial soil C losses with warming and an important positive feedback to climate change³³. Our results also show that, although C contents and stocks in arid and cold grasslands and shrublands are lower than those in the tropical and temperate forests evaluated, they are predominantly protected by minerals, and therefore relatively more stable against microbial decomposition and elevated temperatures at a millennial scale^{34,35}.

Biotic and abiotic drivers of C storage in different fractions during soil development.

Given the important reported changes in the proportion of C associated with different fractions across ecosystems, we conducted structural equation modeling (SEM, Fig. 3) to investigate the major environmental drivers of the mineral protection of surface soil C. The spatial autocorrelation in our database was accounted for by including the geographical

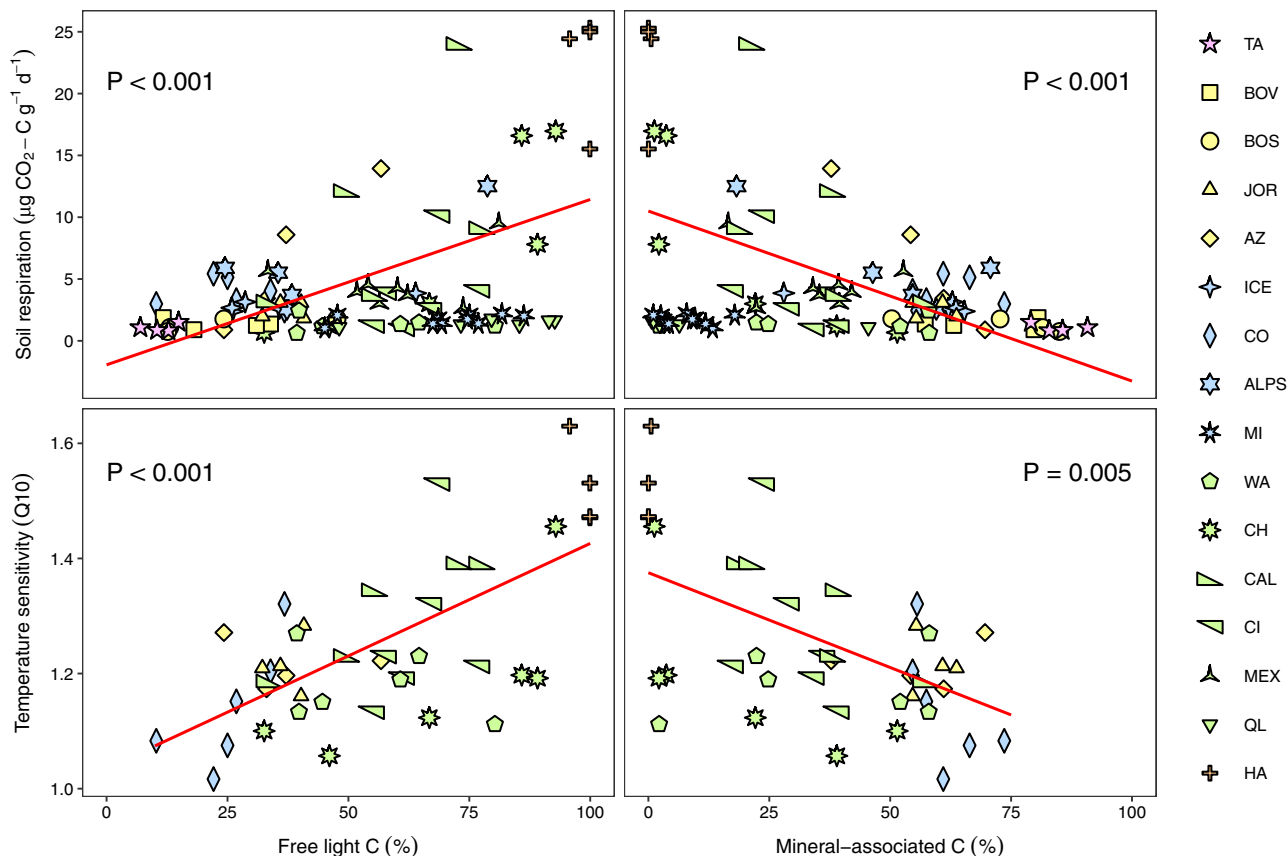


Fig. 2 Relationship between the proportion of free light and mineral-associated carbon fractions and soil respiration and temperature sensitivity of soil respiration. Red lines represent predicted values adjusted for net primary productivity and fine texture. Each panel shows the *p* value for the effect of the corresponding carbon (C) fraction in a linear mixed-effects model that include net primary productivity and fine texture as covariates. Proportion of C fraction *i* (%) = C fraction *i* content × 100/sum of all C fraction contents.

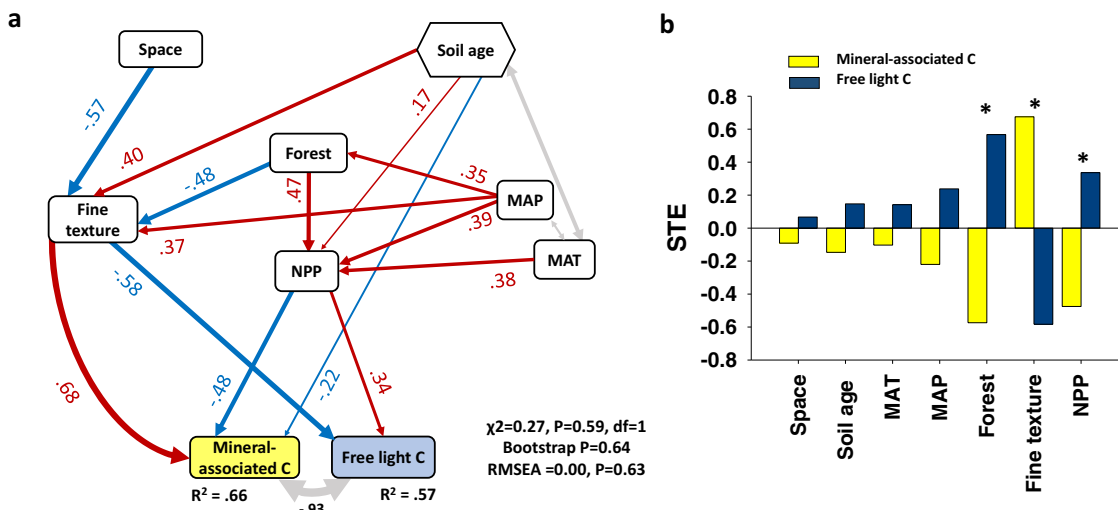


Fig. 3 Abiotic and biotic factors controlling the proportion of surface soil free light and mineral-associated carbon fractions across biomes. **a** includes a structural equation model (SEM) of significant relationships among variables (*p* < 0.05) determining the proportion of carbon (C) fractions. Red and blue arrows represent positive and negative relationships, respectively, and their thicknesses the strength of the relationship. Numbers adjacent to arrows are standardized path coefficients, indicative of the sign and strength of the relationships among the variables. **b** shows the standardized total (direct + indirect) effects (STE) of abiotic and biotic predictors on the proportion of C fractions. MAT mean annual temperature, MAP mean annual precipitation, NPP (NDVI) plant productivity. Information on the direct effects for other SEM arrows can be found in Supplementary Table 2. **p* < 0.05. Proportion of C fraction *i* (%) = C fraction *i* content × 100/sum of all C fraction contents. See text and Supplementary Data 1 for information on the chronosequences.

distance across all plots in our model design (space) (see Methods and Supplementary Table 1 for details on this and other variables). We found that contemporary levels of ecosystem productivity (as measured with the Normalized Difference Vegetation Index (NDVI)) and soil fine texture (% of clay and silt) were the main factors explaining the vast differences in the proportion of free light and mineral-associated C fractions across ecosystems (Fig. 3). Our analysis showed that higher precipitation, higher temperature and forest vegetation resulted in greater levels of ecosystem productivity (Fig. 3). Soil C in highly productive ecosystems was predominantly stored in the free light organic matter fraction (Fig. 3 and Supplementary Figs. 2–6; but see TA in Fig. 1). In contrast, soil C in less productive environments was mainly stored in the mineral-associated organic matter fraction, which was significantly and positively associated with fine texture content, and indirectly associated with soil age (Fig. 3 and Supplementary Figs. 5 and 6).

Limitations and implications. While our findings contribute toward a more comprehensive understanding of the changes and drivers of soil C fractions during soil development across a wide range of chronosequences, it is important to note that they cannot be extrapolated directly to infer changes in soil C storage globally^{9,19,25,26}. Further, the implications of our study can only be extended to the surface soil layer (0–10 cm) and not to total C stocks of the whole soil profile⁹. Our data from globally distributed chronosequences indicate that mineral protection of surface soil C changes relatively little with soil development, but varies considerably across terrestrial ecosystems. Soil age alone, however, may not be an accurate proxy for the progression of mineral weathering, which strongly depends on parent material, and even though we used well-established soil chronosequences, the occurrence of regressive processes (i.e., erosion) cannot be discarded without specific mineralogical data. Broad climatic and ecosystem drivers of soil organic C storage may also mask site-specific changes attributable to soil geochemistry³⁶. In fact, it is noteworthy that previous single-chronosequence studies indicated that C stabilization in the surface soil of dry ecosystems, and in deeper soil layers of moist ecosystems, is largely driven by soil mineralogy and weathering^{9,19}. Weathering controls the formation and availability of reactive mineral surfaces that can stabilize C through sorption or formation of aggregates¹⁹. As such, the amount of C stored in deeper soil layers in temperate and tropical systems and associated with minerals might also be less vulnerable to microbial decomposition as soil ages prior to ecosystem retrogression. While our approach enabled comparison of factors driving soil C contents across soil surface and across different ecosystems, it did not allow us to estimate how soil depth interacted with soil age to influence soil C stabilization, which remains a future challenge.

Conclusions

In summary, our work demonstrates that mineral protection of surface soil C varies considerably across ecosystem types, but not that much as soil develops from centuries to millennia in a wide range of environmental contexts. We found that soil C in warm and wet forest ecosystems is predominantly stored in free organic matter fractions as soil develops, and that these soils are highly vulnerable to reductions in ecosystem productivity and warming temperatures. In contrast, soil C in cold and arid ecosystems is mainly stored in mineral-associated organic matter fractions during soil development, and is mainly driven by soil texture and far less vulnerable to warming. Taken together, this research advances our understanding on the dynamics of soil C stability and temperature dependence during soil development.

Methods

Long-term chronosequences. We used a globally distributed set of 16 long-term soil chronosequences located in nine countries from six continents, each consisting of four to ten sites representing an increasing temporal stage during ecosystem development. The chronosequences cover a wide range of parent material (volcanic material, sedimentary rocks, and sand dunes), climates (tropical, temperate, continental, polar, and arid), vegetation (grasslands, shrublands, forests, and croplands), and age gradient (from hundreds to millions of years). Further information of the study sites was provided in^{27,37} and summarized here in Supplementary Fig. 1 and Supplementary Data 1. Climatic type was obtained from the Koppen classification (<http://koeppen-geiger.vu-wien.ac.at/present.htm>)³⁸; here we used the term warm in a broad sense for equatorial, arid and warm temperate climates, and cold for boreal and polar climates sensu the Koppen classification³⁸. Mean annual temperature and precipitation was determined from the WorldClim database (<https://www.worldclim.org>).

Vegetation survey. For each site, we set up a 50 × 50 m plot representative for the spatial heterogeneity of the ecosystem. Total plant cover was determined from data collected in three parallel transects of 50 m, spaced 25 m apart, using the line-intercept method^{27,39}. We used the NDVI as our proxy for plant primary productivity (NPP), referred to as ecosystem productivity throughout the text. This index provides a global measure of the “greenness” of vegetation across Earth’s landscapes for a given composite period, and has been widely used to quantify NPP in large-scale studies^{40–42}. Data were obtained from the Moderate Resolution Imaging Spectroradiometer (MODIS) aboard NASA’s Terra satellites (<http://neo.sci.gsfc.nasa.gov/>), which provides data 23 times per year with a pixel size of 250 m × 250 m. We calculated the mean value of NDVI index from monthly data (2008–2017).

Soil sampling. We collected five soil core samples under the dominant vegetation type of each plot (a total of 435 soil samples) with an open-tube sampler to avoid compaction. Each soil sample consisted of a composite of five cores taken from a depth of 0 to 10 cm (topsoil; excluding litter/plant debris from the soil surface). This sampling depth, which is consistent with previous works on soil C storage across spatiotemporal scales^{19,21,30}, was suitable since a number of the study sites (e.g., youngest sites in volcanic chronosequences) are very shallow, which does not allow deeper sampling and a comparative analysis of deeper layers across all chronosequences. The topsoil is the most biologically active layer²⁹, has the largest concentration of organic C along the soil profile and is particularly important in a context of climate and land use change^{1,30,43}. Bulk density was calculated as the dry mass of the soil sample divided by its volume in the field. Prior to further analysis, the soil samples were passed through a 2-mm sieve. A portion of each soil sample was air-dried and used for chemical analysis and soil organic matter fractionation, whereas another portion was stored at –20 °C and used for biological analysis²⁷. Each soil analysis was conducted in the same laboratory. Fine texture (% clay + silt) was determined on air-dried samples by sieving and sedimentation⁴⁴.

Soil organic C analysis and fractionation. We analyzed the 435 soil samples for total organic C content by colorimetry after oxidation with K₂Cr₂O₇ and H₂SO₄ at 150 °C for 30 min⁴⁵ at the Biology and Geology Department of Rey Juan Carlos University (Móstoles, Spain). One of the composite soil samples of each study site was fractionated to isolate soil organic C pools characterized by different mechanisms of stability and protection from decomposition. We used the well-established density-based fractionation scheme developed by ref. 28 with slight modifications^{46,47}. This scheme is widely used in soil organic matter research^{15,48} and is intended to isolate three soil organic matter fractions directly connected to conceptual mechanisms of stabilization: a free light fraction organic matter, located between soil aggregates and accessible to microbial decomposers; an occluded, intra-aggregate light fraction organic matter, physically protected by occlusion within soil aggregates and disconnection from decomposers; and a mineral-associated organic matter fraction, chemically protected from decomposition by sorption to mineral surfaces and, consequently, with longer turnover times than free and intra-aggregate fractions.

Briefly, we added 40 ml of NaI at a density of 1.85 g ml^{–1} to 4 g of soil in a 50-ml centrifuge tube. The centrifuge tube was rotated at 1 revolution s^{–1} for 30 s in an overhead shaker. After centrifugation at 2500 × g for 30 min, the floating (free) light fraction was separated from the heavy fraction by suction and filtration through a glass fiber filter and washed with deionized water. The NaI solution was added to the heavy fraction in the centrifuge tube, and the mixture was sonicated at an energy input of 1500 J g^{–1} (calibrated calorimetrically^{49–51}). The floating light (occluded) fraction was separated from the heavy (mineral-associated) fraction by centrifugation at 2500 × g for 60 min, suction, and filtration through a glass fiber filter, and washed with deionized water. We used a density of 1.85 g ml^{–1} and a dispersion energy of 1500 J g^{–1} for consistency with previous studies^{46,52–54}.

The three isolated fractions were oven-dried at 60 °C, weighed, ground with a ball mill and analyzed for organic C concentration by dry combustion and gas chromatography using a Thermo Scientific Flash 2000 CN analyzer (Thermo Fisher Scientific, MA). In the case of the mineral-associated organic matter fraction, the organic C concentration was determined after acid fumigation to

remove carbonates⁵⁵. Soil organic matter fractionation and C concentration analysis of the isolated fractions were performed at the Institute of Agricultural Sciences of the Spanish National Research Council (CSIC, Madrid, Spain). We found a high correlation between the sum of free light, occluded light and mineral-associated C and the total organic C content analyzed on whole soil samples colorimetrically as described above ($r = 0.987$, $p < 0.001$, $n = 87$). The median (interquartile range) C recovery (sum of C content recovered in free light, occluded light and mineral-associated C fractions relative to the total organic C content) was 89.4 (34.5)%. We found no significant differences in C recovery based on parent material nor between high and low productive ecosystems (Kruskal-Wallis rank sum tests, $p = 0.669$ and 0.368 , respectively).

We estimated the stocks of total organic C and its free light, occluded light and mineral-associated fractions (kg C m^{-2}) as the product of sampling depth, C content (g C kg^{-1} soil) and bulk density (Supplementary Fig. 2). Bulk density was calculated as the dry weight of the soil sample collected with the core cylinder divided by its volume, assuming negligible coarse fraction (>2 mm) contents. The quantification of changes in soil C stocks to a fixed depth over time, however, requires that soil bulk density does not change through time. This is because the same depths at different times correspond to equivalent soil mass and layers only if bulk density remains constant²¹. Since this condition was not met in our chronosequences, we focused our analyses mainly on the content and proportion of soil organic C fractions (proportion of organic C fraction $i = \text{organic C fraction } i \text{ content} \times 100 / \text{sum of all organic C fraction contents}$) rather than the stocks.

To address whether our results were contingent on the fractionation method used (density-based), we repeated the analysis on a subset of samples across contrasting chronosequences ($n = 24$) using a size fractionation method, which is also widely used in soil organic matter research^{15,18,56}. In particular, we used an automated wet sieving system to separate particulate organic matter ($>53 \mu\text{m}$) from mineral-associated soil organic matter ($<53 \mu\text{m}$) after dispersion with sodium hexametaphosphate. The free light C separated by density was highly correlated with the particulate organic C separated by size ($r = 0.975$, $p < 0.001$), and the same was found for the mineral-associated C fraction ($r = 0.687$, $p < 0.001$) (Supplementary Fig. 7). This cross-validation supports previous findings suggesting that the light fraction separated by density is similar to the particulate organic matter fraction separated by size^{15,18}. In agreement with previous results⁴⁷, the choice of heavy liquid may affect the proportion of occluded and mineral-associated organic C. In particular, compared to NaI solutions, less viscous liquids such as sodium polytungstate solutions may result in greater intra-aggregate and smaller mineral-associated organic C concentrations, because of a greater effectiveness of the ultrasonic disruption treatment to break up aggregates and the release of intra-aggregate C, which in turn decreases the amount of C recovered in the mineral-associated C pool. Also in agreement with previous observations⁴⁷, this bias may be expected to be systematic and operate in the same direction across soils, and thus not to affect our interpretation and discussion on the evolution and drivers of soil C fractions across ecosystems.

Biological soil analysis. We measured soil basal heterotrophic respiration to examine soil biological activity across chronosequences. This analysis was conducted on a composite soil sample per plot by quantifying the total CO_2 released over 16 days from 1 g of bulk soil incubated in the dark at 28°C and 50% water holding capacity in 20-mL glass vials, after a 1-week-long pre-incubation period. These incubation conditions were within the ranges found in the literature to measure soil basal respiration⁵⁷. In addition to these determinations, we measured the potential response of soil heterotrophic respiration to temperature (Q_{10}) to assess the vulnerability of soil C losses to warming. The temperature sensitivity of the soil microbial respiration (Q_{10}) was determined on a composite soil sample per soil age (location) from a subset of eight chronosequences selected to cover a wide range of global environmental conditions in terms of climate, vegetation types and soil age. The Q_{10} coefficient represents the increase in soil respiration as temperature increases by 10°C , and is commonly used to assess warming effects on soil C losses and to model soil C dynamics^{58–60}. Soil respiration rates were measured after short-term (10 h) incubations in triplicate at three increasing temperatures (5, 15 and 25°C) in 96 deep well microplates⁶¹, using the MicroResp technique⁶². We then calculated the β and R_0 coefficients for the exponential relationship between heterotrophic soil respiration rate (R_s in $\mu\text{g CO}_2\text{-C g}^{-1} \text{h}^{-1}$) and temperature (T , in $^\circ\text{C}$): $R_s = R_0 \times \exp(\beta \times T)$; and used β to compute Q_{10} using the equation $Q_{10} = \exp(10 \times \beta)$. The MicroResp technique has been successfully used in previous studies for high-throughput quantification of Q_{10} values⁶¹. Higher soil respiration rates and Q_{10} values were interpreted as higher soil C vulnerability to microbial decomposition and increases in temperature. We used short incubations to prevent microbial acclimation to the assay temperature used in the laboratory^{63–65}. We acknowledge that C respired during incubations may also represent chemically labile old C that is physically protected in the field but is freed during soil sampling and sieving in the lab⁶⁶.

Data analysis. The effects of ecosystem productivity, soil age (binned in three arbitrary categories: thousands of years, hundreds of thousand years and millions of years) and their interaction were analyzed by linear mixed-effects models, with an intercept structure in the random term to account for the lack of independence among soils from the same chronosequence. We excluded a subtropical chronosequence in an area naturally dominated by broad-leaved evergreen forests in

Taiwan (TA) from this analysis, because its natural productivity was altered being cropped with tea for the last 100 years. Normality and homoscedasticity were examined visually using residual plots. The relationships between soil respiration and temperature sensitivity of soil respiration and the relative abundance of free light and mineral-associated C fractions were also assessed with linear mixed-effects modeling, including net primary productivity (evaluated with the NDVI index) and fine texture (percentage of clay and silt) as covariates. P values for fixed effects were computed via the Satterthwaite approximation. We used SEM⁶⁷ to examine the complex (direct and indirect) effects of climate, vegetation, soil age, soil properties on the proportion of free light and mineral-associated soil organic C. For soil age, we used a standardized composite variable created from three complementary metrics: a quantitative index of soil age (years; $\log_{10} + 1$ -transformed), a semi-quantitative index of age range (i.e., thousands of years, hundreds of thousand years and millions of years) and a qualitative soil age index (standardized soil age range from 0 to 1 calculated for each chronosequence following approaches used in previous works⁶⁸). We first created an a priori model that incorporated all potential relationships between variables based on prior ecological knowledge (Supplementary Fig. 8). We included a geographical variable (space) created from the coordinates and distances between sites to account for spatial dependencies and information redundancy. The statistical analysis and plots were performed using IBM SPSS v. 26⁶⁹, R⁷⁰ and the R packages ggeffects⁷¹, ggnewscale⁷², ggstar⁷³, ggtext⁷⁴, lme4⁷⁵, lmerTest⁷⁶, patchwork⁷⁷, readxl⁷⁸, rgeos⁷⁹, rnaturlaearth⁸⁰, tidyverse⁸¹.

Reporting summary. Further information on research design is available in the Nature Research Reporting Summary linked to this article.

Data availability

The data associated with this study are publicly available in Figshare (<https://doi.org/10.6084/m9.figshare.12619466>).

Received: 25 November 2021; Accepted: 28 September 2022;

Published online: 07 October 2022

References

- Jackson, R. B. et al. The ecology of soil carbon: pools, vulnerabilities, and biotic and abiotic controls. *Annu. Rev. Ecol. Syst.* **48**, 419–445 (2017).
- Paul, E. A. The nature and dynamics of soil organic matter: plant inputs, microbial transformations, and organic matter stabilization. *Soil. Biol. Biochem.* **98**, 109–126 (2016).
- Amundson, R. et al. Soil and human security in the 21st century. *Science* **348**, 1261071–1261071 (2015).
- Batjes, N. H. Harmonized soil property values for broad-scale modelling (WISE30sec) with estimates of global soil carbon stocks. *Geoderma* **269**, 61–68 (2016).
- Crowther, T. W. et al. The global soil community and its influence on biogeochemistry. *Science* **365**, eaav0550 (2019).
- Hengl, T. et al. SoilGrids250m: global gridded soil information based on machine learning. *PLoS ONE* **12**, e0169748 (2017).
- Schlesinger, W. H. Evidence from chronosequence studies for a low carbon-storage potential of soils. *Nature* **348**, 232–234 (1990).
- Peltzer, D. A. et al. Understanding ecosystem retrogression. *Ecol. Monogr.* **80**, 509–529 (2010).
- Torn, M. S., Trumbore, S. E., Chadwick, O. A., Vitousek, P. M. & Hendricks, D. M. Mineral control of soil organic carbon storage and turnover. *Nature* **389**, 170–173 (1997).
- Kleber, M. et al. Mineral–organic associations: formation, properties, and relevance in soil environments. in *Advances in Agronomy* (ed. Sparks, D. L.) 130 1–140 (Academic Press, 2015).
- Kleber, M. et al. Dynamic interactions at the mineral–organic matter interface. *Nat. Rev. Earth Environ.* <https://doi.org/10.1038/s43017-021-00162-y> (2021).
- Schmidt, M. W. I. et al. Persistence of soil organic matter as an ecosystem property. *Nature* **478**, 49–56 (2011).
- Lehmann, J. & Kleber, M. The contentious nature of soil organic matter. *Nature* **528**, 60–68 (2015).
- Hemingway, J. D. et al. Mineral protection regulates long-term global preservation of natural organic carbon. *Nature* **570**, 228–231 (2019).
- Lavallee, J. M., Soong, J. L. & Cotrufo, M. F. Conceptualizing soil organic matter into particulate and mineral-associated forms to address global change in the 21st century. *Glob. Chang. Biol.* **26**, 261–273 (2020).
- Liu, X. J. A., Frey, S. D., Melillo, J. M. & DeAngelis, K. M. Physical protection regulates microbial thermal responses to chronic soil warming. *Soil. Biol. Biochem.* **159**, 108298 (2021).

17. Lugato, E., Lavalée, J. M., Haddix, M. L., Panagos, P. & Cotrufo, M. F. Different climate sensitivity of particulate and mineral-associated soil organic matter. *Nat. Geosci.* <https://doi.org/10.1038/s41561-021-00744-x> (2021).
18. Mikutta, R. et al. Microbial and abiotic controls on mineral-associated organic matter in soil profiles along an ecosystem gradient. *Sci. Rep.* **9**, 10294 (2019).
19. Doetterl, S. et al. Links among warming, carbon and microbial dynamics mediated by soil mineral weathering. *Nat. Geosci.* **11**, 589–593 (2018).
20. Cotrufo, M. F., Ranalli, M. G., Haddix, M. L., Six, J. & Lugato, E. Soil carbon storage informed by particulate and mineral-associated organic matter. *Nat. Geosci.* **12**, 989–994 (2019).
21. Doetterl, S. et al. Soil carbon storage controlled by interactions between geochemistry and climate. *Nat. Geosci.* **8**, 780–783 (2015).
22. Masiello, C. A., Chadwick, O. A., Southon, J., Torn, M. S. & Harden, J. W. Weathering controls on mechanisms of carbon storage in grassland soils. *Glob. Biogeochem. Cycles* **18**, 1–9 (2004).
23. Lawrence, C. R., Harden, J. W., Xu, X., Schulz, M. S. & Trumbore, S. E. Long-term controls on soil organic carbon with depth and time: a case study from the Cowlitz River Chronosequence, WA USA. *Geoderma* **247–248**, 73–87 (2015).
24. Rasmussen, C. et al. Controls on soil organic carbon partitioning and stabilization in the California sierra nevada. *Soil. Syst.* **2**, 1–18 (2018).
25. Baisden, W. T. et al. A multiisotope C and N modeling analysis of soil organic matter turnover and transport as a function of soil depth in a California annual grassland soil chronosequence. *Glob. Biogeochem. Cycles* **16**, 82–182–26 (2002).
26. Baisden, W. T., Amundson, R., Cook, A. C. & Brenner, D. L. Turnover and storage of C and N in five density fractions from California annual grassland surface soils. *Glob. Biogeochem. Cycles* **16**, 64–164–16 (2002).
27. Delgado-Baquerizo, M. et al. Changes in belowground biodiversity during ecosystem development. *Proc. Natl. Acad. Sci. USA* **116**, 6891–6896 (2019).
28. Golchin, A., Oades, J. M., Skjemstad, J. O. & Clarke, P. Soil structure and carbon cycling. *Aust. J. Soil. Res.* **32**, 1043–1063 (1994).
29. Rey, A., Pegoraro, E. & Jarvis, P. G. Carbon mineralization rates at different soil depths across a network of European forest sites (FORCAST). *Eur. J. Soil. Sci.* **59**, 1049–1062 (2008).
30. Crowther, T. W. et al. Quantifying global soil carbon losses in response to warming. *Nature* **540**, 104–108 (2016).
31. Ellert, B. H., Janzen, H. H., VandenBygaart, A. J. & Bremer, E. Measuring change in soil organic carbon storage. in *Soil Sampling and Methods of Analysis* (eds. Carter, M. R. & Gregorich, E. G.) 25–38 (CRC Press, 2007).
32. Tsai, H., Huang, W. S., Hseu, Z. Y. & Chen, Z. S. A river terrace soil chronosequence of the Pakua tableland in central Taiwan. *Soil. Sci.* **171**, 167–179 (2006).
33. Nottingham, A. T., Meir, P., Velasquez, E. & Turner, B. L. Soil carbon loss by experimental warming in a tropical forest. *Nature* **584**, 234–237 (2020).
34. Giardina, C. P. & Ryan, M. G. Evidence that decomposition rates of organic carbon in mineral soil do not vary with temperature. *Nature* **404**, 858–861 (2000).
35. Qin, S. et al. Temperature sensitivity of SOM decomposition governed by aggregate protection and microbial communities. *Sci. Adv.* **5**, eaau1218 (2019).
36. Nave, L. E. et al. Patterns and predictors of soil organic carbon storage across a continental-scale network. *Biogeochemistry* <https://doi.org/10.1007/s10533-020-00745-9> (2021).
37. Delgado-Baquerizo, M. et al. The influence of soil age on ecosystem structure and function across biomes. *Nat. Commun.* **11**, 4721 (2020).
38. Kottek, M., Grieser, J., Beck, C., Rudolf, B. & Rubel, F. World map of the Köppen-Geiger climate classification updated. *Meteorol. Z.* **15**, 259–263 (2006).
39. Maestre, F. T. et al. Plant species richness and ecosystem multifunctionality in global drylands. *Science* **335**, 214–218 (2012).
40. Paruelo, J. M., Epstein, H. E., Lauenroth, W. K. & Burke, I. C. ANPP estimates from NDVI for the Central Grassland Region of the United States. *Ecology* **78**, 953 (1997).
41. Running, S. W. Estimating terrestrial primary productivity by combining remote sensing and ecosystem simulation. in *Remote Sensing of Biosphere Functioning* (eds. Hobbs, R. J. & Mooney, H. A.) 65–86 (Springer, 1990).
42. Rafique, R., Zhao, F., De Jong, R., Zeng, N. & Asrar, G. R. Global and regional variability and change in terrestrial ecosystems net primary production and NDVI: a model-data comparison. *Remote Sens.* **8**, 177 (2016).
43. Jobbágy, E. G. & Jackson, R. B. The vertical distribution of soil organic carbon and its relation to climate and vegetation. *Ecol. Appl.* **10**, 423–436 (2000).
44. Kettler, T. A., Doran, J. W. & Gilbert, T. L. Simplified method for soil particle-size determination to accompany soil-quality analyses. *Soil. Sci. Soc. Am. J.* **65**, 849–852 (2001).
45. Baillie, I. C., Anderson, J. M. & Ingram, J. S. I. *Tropical Soil Biology and Fertility. A Handbook of Methods* 78 (C.A.B. International, 1990).
46. Sohi, S. P. et al. A procedure for isolating soil organic matter fractions suitable for modeling. *Soil. Sci. Soc. Am. J.* **65**, 1121–1128 (2001).
47. Plaza, C., Giannetta, B., Benavente, I., Vischetti, C. & Zaccone, C. Density-based fractionation of soil organic matter: effects of heavy liquid and heavy fraction washing. *Sci. Rep.* **9**, 10146 (2019).
48. Gosling, P., Parsons, N. & Bending, G. D. What are the primary factors controlling the light fraction and particulate soil organic matter content of agricultural soils? *Biol. Fertil. Soils* **49**, 1001–1014 (2013).
49. North, P. F. Towards an absolute measurement of soil structural stability using ultrasound. *J. Soil. Sci.* **27**, 451–459 (1976).
50. Oorts, K., Vanlauwe, B., Recous, S. & Merckx, R. Redistribution of particulate organic matter during ultrasonic dispersion of highly weathered soils. *Eur. J. Soil. Sci.* **56**, 77–91 (2005).
51. Roscoe, R., Buurman, P. & Velthorst, E. J. Disruption of soil aggregates by varied amounts of ultrasonic energy in fractionation of organic matter of a clay Latosol: carbon, nitrogen and $\delta^{13}C$ distribution in particle-size fractions. *Eur. J. Soil. Sci.* **51**, 445–454 (2000).
52. Six, J., Elliott, E. T., Paustian, K. & Doran, J. W. Aggregation and soil organic matter accumulation in cultivated and native grassland soils. *Soil. Sci. Soc. Am. J.* **62**, 1367–1377 (1998).
53. Six, J., Elliott, E. T. & Paustian, K. Aggregate and soil organic matter dynamics under conventional and no-tillage systems. *Soil. Sci. Soc. Am. J.* **63**, 1350–1358 (1999).
54. Six, J., Paustian, K., Elliott, E. T. & Combrink, C. Soil structure and organic matter: I. Distribution of aggregate-size classes and aggregate-associated carbon. *Soil. Sci. Soc. Am. J.* **64**, 681–689 (2000).
55. Harris, D., Horwath, W. R. & Van Kessel, C. Acid fumigation of soils to remove carbonates prior to total organic carbon or carbon-13 isotopic analysis. *Soil. Sci. Soc. Am. J.* **65**, 1853–1856 (2001).
56. Sokol, N. W. & Bradford, M. A. Microbial formation of stable soil carbon is more efficient from belowground than aboveground input. *Nat. Geosci.* **12**, 46–53 (2019).
57. Creamer, R. E. et al. Measuring basal soil respiration across Europe: do incubation temperature and incubation period matter? *Ecol. Indic.* **36**, 409–418 (2014).
58. Melillo, J. M. et al. Long-term pattern and magnitude of soil carbon feedback to the climate system in a warming world. *Science* **358**, 101–105 (2017).
59. Carey, J. C. et al. Temperature response of soil respiration largely unaltered with experimental warming. *Proc. Natl. Acad. Sci. USA* **113**, 13797–13802 (2016).
60. Meyer, N., Welp, G. & Amelung, W. The temperature sensitivity (Q10) of soil respiration: controlling factors and spatial prediction at regional scale based on environmental soil classes. *Glob. Biogeochem. Cycles* **32**, 306–323 (2018).
61. Dacal, M., Bradford, M. A., Plaza, C., Maestre, F. T. & García-Palacios, P. Soil microbial respiration adapts to ambient temperature in global drylands. *Nat. Ecol. Evol.* **3**, 232–238 (2019).
62. Campbell, C. D., Chapman, S. J., Cameron, C. M., Davidson, M. S. & Potts, J. M. A rapid microtiter plate method to measure carbon dioxide evolved from carbon substrate amendments so as to determine the physiological profiles of soil microbial communities by using whole soil. *Appl. Environ. Microbiol.* **69**, 3593–3599 (2003).
63. Bradford, M. A., Watts, B. W. & Davies, C. A. Thermal adaptation of heterotrophic soil respiration in laboratory microcosms. *Glob. Chang. Biol.* **16**, 1576–1588 (2010).
64. Bradford, M. A. et al. Cross-biome patterns in soil microbial respiration predictable from evolutionary theory on thermal adaptation. *Nat. Ecol. Evol.* **3**, 223–231 (2019).
65. Tucker, C. L., Bell, J., Pendall, E. & Ogle, K. Does declining carbon-use efficiency explain thermal acclimation of soil respiration with warming? *Glob. Chang. Biol.* **19**, 252–263 (2013).
66. Ewing, S. A., Sanderman, J., Baisden, W. T., Wang, Y. & Amundson, R. Role of large-scale soil structure in organic carbon turnover: Evidence from California grassland soils. *J. Geophys. Res. Biogeosci.* **111**, G03012 (2006).
67. Grace, J. B. *Structural Equation Modeling and Natural Systems* (Cambridge University Press, 2006).
68. Laliberté, E. et al. Soil fertility shapes belowground food webs across a regional climate gradient. *Ecol. Lett.* **20**, 1273–1284 (2017).
69. IBM Corp. *IBM SPSS Statistics for Macbook* (IBM Corp, 2017).
70. R Core Team. *R: A Language and Environment for Statistical Computing* (R Core Team, 2021).
71. Lüdtke, D. ggeffects: tidy data frames of marginal effects from regression models. *J. Open. Source Softw.* **3**, 772 (2018).
72. Campitelli, E. ggnewscale: multiple fill and colour scales in 'ggplot2'. (2022).
73. Xu, S. ggstat: multiple geometric shape point layer for 'ggplot2'. (2021).
74. Wilke, C. O. ggtext: improved text rendering support for 'ggplot2'. R package version 0.1.1. (2020).
75. Bates, D., Mächler, M., Bolker, B. M. & Walker, S. C. Fitting linear mixed-effects models using lme4. *J. Stat. Softw.* **67**, 1–48 (2015).
76. Kuznetsova, A., Brockhoff, P. B. & Christensen, R. H. B. lmerTest Package: tests in linear mixed effects models. *J. Stat. Softw.* **82**, 1–26 (2017).

77. Pedersen, T. L. patchwork: the Composer of Plots. R package version 1.1.1. <https://CRAN.R-project.org/package=patchwork>. (2020).
78. Wickham, H. & Brian, J. readxl: Read Excel Files (Version 1.3.1). R package version 1.3.1. <https://cran.r-project.org> (2019).
79. Bivand, R. & Rundel, C. rgeos: Interface to Geometry Engine - Open Source ("GEOS"). (2021).
80. South, A. rnatuarearth: world map data from Natural Earth. R package version 0.1.0. The R Foundation. <https://CRAN.R-project.org/package=rnatuarearth> (2017).
81. Wickham, H. et al. Welcome to the Tidyverse. *J. Open. Source Softw.* **4**, 1686 (2019).

Acknowledgements

M.D.-B. and P.G.-P. were supported by Ramón y Cajal grants from the Spanish Ministry of Science and Innovation (RYC2018-025483-I and RYC2018-024766-I). This project received funding from the European Union's Horizon 2020 research and innovation program under the Marie Skłodowska-Curie grant agreement 702057 and the Spanish State Plan for Scientific and Technical Research and Innovation (2013–2016), award ref. AGL201675762-R (AEI/FEDER, UE). M.D.-B. acknowledges support from the Spanish Ministry of Science and Innovation for the I+D+i project PID2020-115813RA-I00 funded by MCIN/AEI/10.13039/501100011033. M.D.-B. is also supported by a project of the Fondo Europeo de Desarrollo Regional (FEDER) and the Consejería de Transformación Económica, Industria, Conocimiento y Universidades of the Junta de Andalucía (FEDER Andalucía 2014–2020 Objetivo temático "01—Refuerzo de la investigación, el desarrollo tecnológico y la innovación") associated with the research project P20_00879 (ANDABIOMA). C.P. acknowledges support from the EU H2020 research and innovation programme under grant agreement No 101000224. F.B. acknowledges support from CSIC i-LINK + 2018 (LINKA20069), PID2020-114942RB-I00 funded by MCIN/AEI/10.13039/501100011033 and Fundación Séneca from Murcia Province (19896/GERM/15). We thank the researchers involved in the CLIMIFUN project for collection of field data and soil samples. We would like to thank Fernando Maestre, Victoria Ochoa and Beatriz Gozalo for their help with lab analyses, Lynn Riedel, Julie Larson, Katy Waechter and Drs. David Buckner and Brian Anacker for their help with soil sampling in the chronosequence from Colorado, and to the City of Boulder Open Space and Mountain Parks for allowing us to conduct these collections. We also thank Melissa Martin for revising the English in this manuscript. We also thank Dr. Santiago Soliveres (University of Alicante, Spain) and Dr. Miguel Berdugo (Pompeu Fabra University, Spain) for helpful comments on an earlier version of the manuscript.

Author contributions

M.D.-B., C.P. and P.G.-P. designed the study presented in the manuscript. M.D.-B. devised the chronosequence survey and coordinated all the research activities. C.P.,

P.G.-P., J.B., F.B., G.K.P., A.R. and M.D.-B. conducted laboratory research. M.D.-B., P.G.-P. and C.P. performed data analysis. C.P., P.G.-P., A.A.B., J.B., F.B., G.K.P., A.R., R.D.B. and M.D.-B. substantially discussed the results. C.P., M.D.-B. and P.G.-P. wrote the initial draft of the manuscript, and A.A.B., J.B., F.B., G.K.P., A.R. and R.D.B. significantly contributed to editing.

Competing interests

The authors declare no competing interests.

Additional information

Supplementary information The online version contains supplementary material available at <https://doi.org/10.1038/s43247-022-00567-7>.

Correspondence and requests for materials should be addressed to César Plaza or Manuel Delgado-Baquerizo.

Peer review information *Communications Earth & Environment* thanks Wenjuan Huang and the other, anonymous, reviewer(s) for their contribution to the peer review of this work. Primary Handling Editors: Erika Buscardo and Clare Davis.

Reprints and permission information is available at <http://www.nature.com/reprints>

Publisher's note Springer Nature remains neutral with regard to jurisdictional claims in published maps and institutional affiliations.



Open Access This article is licensed under a Creative Commons Attribution 4.0 International License, which permits use, sharing, adaptation, distribution and reproduction in any medium or format, as long as you give appropriate credit to the original author(s) and the source, provide a link to the Creative Commons license, and indicate if changes were made. The images or other third party material in this article are included in the article's Creative Commons license, unless indicated otherwise in a credit line to the material. If material is not included in the article's Creative Commons license and your intended use is not permitted by statutory regulation or exceeds the permitted use, you will need to obtain permission directly from the copyright holder. To view a copy of this license, visit <http://creativecommons.org/licenses/by/4.0/>.

© The Author(s) 2022